Low-Level Laser Therapy Decreases Renal Interstitial Fibrosis

Fabiana Aparecida Mayrink Oliveira, M.D.,[1,2] Ana Carolina Meneghin Moraes, M.D.,[1,2]
Amanda Povoa Paiva, M.D.,[1,2] Vânia Schinzel, M.D.,[1,2] Matheus Correa-Costa, Ph.D.,[3,4]
Patricia Semedo, Ph.D.,[4] Angêla Castoldi, B.S., M.Sc.,[4] Marcos Antonio Cenedeze,[4]
Roberto Sotto-Maior Fortes Oliveira, Ph.D.,[2] Marcus Gomes Bastos, M.D., Ph.D.,[1]
Niels Olsen Saraiva Câmara, M.D., Ph.D.,[3,4] and Helady Sanders-Pinheiro, M.D., Ph.D.[1–4]

Abstract

Objective: the purpose of this study was to investigate the effect of low-level laser therapy (LLLT) on chronic kidney disease (CKD) in a model of unilateral ureteral obstruction (UUO). *Background data:* Regardless of the etiology, CKD involves progressive widespread tissue fibrosis, tubular atrophy, and loss of kidney function. This process also occurs in kidney allograft. At present, effective therapies for this condition are lacking. We investigated the effects of LLLT on the interstitial fibrosis that occurs after experimental UUO in rats. *Methods:* The occluded kidney of half of the 32 Wistar rats that underwent UUO received a single intraoperative dose of LLLT (AlGaAs laser, 780 nm, 22.5 J/cm^2, 30 mW, 0.75 W/cm^2, 30 sec on each of nine points). After 14 days, renal fibrosis was assessed by Sirius red staining under polarized light. Immunohistochemical analyses quantitated the renal tissue cells that expressed fibroblast (FSP-1) and myofibroblast (α-SMA) markers. Reverse transcriptase polymerase chain reaction (RT-PCR) was performed to determine the mRNA expression of interleukin (IL)-6, monocyte chemotactic protein-1 (MCP-1), transforming growth factor (TGF)-β1 and Smad3. *Results:* The UUO and LLLT animals had less fibrosis than the UUO animals, as well having decreased expression inflammatory and pro-fibrotic markers. *Conclusions:* For the first time, we showed that LLLT had a protective effect regarding renal interstitial fibrosis. It is conceivable that by attenuating inflammation, LLLT can prevent tubular activation and transdifferentiation, which are the two processes that mainly drive the renal fibrosis of the UUO model.

Introduction

CHRONIC KIDNEY DISEASE (CKD) is a devastating condition and a global public health problem. In the more advanced stage of CKD, patients become dependent on life-long dialysis treatment or require renal transplantation. The human and economic impact of CKD is enormous.[1]

Regardless of the etiology, the pathogenesis of CKD always results in a persistent chronic inflammation of the kidney tissue by pro-inflammatory mediators such as tumor necrosis factor (TNF)-α, interleukin (IL)-1β, IL-6, monocyte chemotactic protein-1 (MCP-1), and osteopontin.[2,3] The kidneys experience progressive loss of function and interstitial fibrosis/tubular atrophy, which is characterized by accumulation of matrix proteins, such as collagen types I and III, metalloproteinases, fibronectin, and vimentin.[4–6]

Some evidence suggests that during renal injury, tubular epithelial cells can differentiate into myofibroblasts that express α-smooth muscle actin (α-SMA) and fibroblasts that express fibroblast-specific protein-1 (FSP1), which is normally expressed by fibroblasts but not epithelial cells: this process is known as tubular epithelial–mesenchymal transition (EMT).[7] The most important of these mediators appears to be the pro-fibrotic molecule transforming growth factor-β1 (TGF-β1).[1] In chronic renal fibrosis, the intracellular signal transduction involved in TGF-β1-induced EMT is

[1]Division of Nephrology, Federal University of Juiz de Fora, Juiz de Fora (UFJF), Brazil.
[2]Center of Reproductive Biology, Federal University of Juiz de Fora, Juiz de Fora (UFJF), Brazil.
[3]Laboratory of Transplantation Immunobiology, Department of Immunology, Institute of Biomedical Sciences IV, University of São Paulo (USP), São Paulo, Brazil.
[4]Laboratory of Clinical and Experimental Immunology, Nephrology Division, Federal University of São Paulo (UNIFESP), São Paulo, Brazil.

accompanied by the upregulation and activation of its Smad effectors.[1,4,5] As a result, the Smads induce fibroblasts to differentiate into myofibroblasts.[7,8]

Unilateral ureteral obstruction (UUO) is a well-established experimental model for the study of the mechanisms behind renal interstitial fibrosis (IF) and for evaluating potential therapeutic approaches that might ameliorate the fibrosis.[9,10] Although most patients with CKD are diagnosed well before they reach end-stage renal failure, effective treatments that can completely halt the progressive decline in renal functions have not yet been developed.[11] Of particular interest in this regard is low-level laser therapy (LLLT), which is widely used in all medical fields because of its dose-dependent ability to induce repair and attenuate the negative consequences of inflammation and fibrosis.[12–16]

LLLT reduces oxidative stress leading to reduced inflammation. LLLT also increases mitochondrial membrane potential, leading to synthesis adenosine triphosphate (ATP) and faster tissue repair.[13, 15–18]

The present study examines whether LLLT can attenuate the renal IF that arises after UUO in rats.

Materials and Methods

Animals and reagents

Thirty-two male Wistar rats aged 8–12 weeks (200–350 g), were obtained from a local colony. The rats were maintained with free access to regular food and water, at $22 \pm 1°C$ under a 12/12 h light/dark cycle. All experimental procedures were conducted according to international ethics guidelines and were previously locally approved (Document number 005/2008).

Experimental and irradiation procedures

We studied four groups of eight animals, named as: sham surgery (Sham), UUO, UUO plus a single dose of LLLT (UUO+L), and sham surgery plus a single dose of LLLT (L). After anesthetizing each animal with 100 mg/kg ketamine and 10 mg/kg xylasine i.p., the UUO was performed by ventral laparotomy. This involved completely ligating the left ureter at two positions with 4-0 silk and then making an incision between the two ligations.[19] Fifteen minutes after UUO, GaAlAs laser irradiation (Twin Laser - MM Optics®, São Carlos, Brazil) was performed at nine points that spanned the surface of the left obstructed kidney. The following LLLT parameters were used: wavelength 780 nm, power output 30 mW, beam area 4 mm², 30 sec at each of the nine points. The delivered energy density was 22.5 J/cm²; in each point. This dose and the administration schedule are based on previous reports, adapted to the specificity of the Twin Laser apparatus.[12,15,20] Animals were kept under normal housing condition until euthanasia at day 14 (Fig. 1).

Preparation of kidney tissue for analysis

On day 14, the rats were anaesthetized as described, the abdominal wall was sectioned, and the left kidney was dissected. First, the kidney was divided into two by a midcoronal section and one half was fixed in buffered 10% formaldehyde solution, embedded in paraffin, stained with Sirius red (F3BA CI 35782, Sigma, St. Louis, MO) and counter-stained with Harris hematoxylin.[21] Second, a small part of the renal cortex was placed in buffered RNAlater®
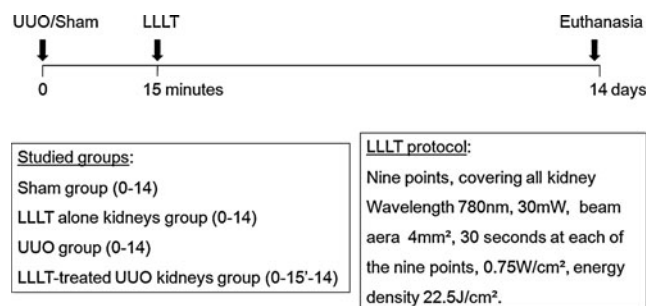

FIG. 1. Experimental design.

(Qiagen, Ambion Inc., Austin, TX) and stored at −80°C for further mRNA analysis. Third, the remaining half of the kidney was fixed for 24 h in Carnoy's fluid and then in 70% methanol, for immunohistochemical studies.

Histomorphometric analysis for renal fibrosis

To evaluate fibrosis, the paraffin-embedded and Sirius red-stained left renal tissue was analyzed by an experienced analyst who was unaware of the source of the sample. The percentage of tissue that was fibrotic was calculated under polarized light using the 20×objective. For this, the slides were examined with an AxioPhot I microscope that was coupled to a ICc3 AxioCam camera, and the AxioVision software v 4.7.2.0 capture system (Carl Zeiss, Goettingen, Germany) was used to acquire the images. The bright Sirius red areas were quantified by using the software ImageJ 1.43a, 64-bit (National Institutes of Health, Bethesda, MD; http://rsbweb.nih.gov/ij). The result of the analysis was represented by percentage, and refers to the proportion of the interstitial volume of collagen in the cortex to the total cortical volume, and then the arithmetic mean of the analyzed fields was calculated for each slide.[21,22] The percentage of positively stained area was counted on 10 consecutive, non-overlapping, 200×fields, of 0.09 mm², per animal. Vessels, glomeruli, the subcapsular cortex, and the medulla were avoided when acquiring the images.

Immunohistochemistry

The left kidney was subjected to immunohistochemical analysis for α-SMA and FSP-1, which are markers of EMT that point to ongoing or established fibrosis. The paraffin-embedded tissue sections were first deparaffinized, rehydrated, and subjected to antigen retrieval and endogenous protein and peroxidase blockages. Thereafter, the slides were incubated with either of the primary antibodies, namely, α-SMA (diluted 1:300; Abcam, Cambrigde, UK) and FSP-1 (diluted 1:600, A5114, DAKO, Ely, UK), or with a negative control reagent. The staining was completed by incubation with 3,3'-diaminobenzidine (DAB).[23]

Light microscopy was performed with a bright field at a magnification of 200× for α-SMA and 400× for FSP-1, by using the same apparatus used for fibrosis analysis. For α-SMA, the percentage of the area that was stained in 20 non-overlapping fields was calculated by using an automated macro specially written for the software package ImageJ 1.43a, 64-bit (National Institutes of Health, Bethesda, MD; http://rsbweb.nih.gov/ij/).[23,24] Vessels, glomeruli, the subcapsular

cortex, and the medulla were again avoided during the image acquisition. The FSP-1 positive cells were counted, manually, also in 20 fields, by using the same software.

Reverse transcriptase polymerase chain reaction (RT- PCR)

Total RNA was isolated from stored kidney tissue by using the TRIzol Reagent (Invitrogen, Carlsbad, CA) and the protocol of the manufacturer. The RNA concentrations were determined by spectrophotometer readings at an absorbance of 260 nm. First-strand cDNAs were synthesized by using MML-V reverse transcriptase (Promega, Madison, WI). RT-PCR was performed by using the SYBR Green real-time PCR assay (Applied Biosystem, Foster City, CA) for the following molecules: MCP-1 (sense) 5-CAGGTCTCTGTCACGCTTCT-3, (antisense) 5-AGTATTCATGGAAGGGAATAG-3; IL-6 (sense) 5- GTGGCTGCAGGACATGACAA-3, (antisense) 5-CAATCTGAGGTGCCCATGCTAC-3; TGF-β1 (sense) 5-TCA GTC CCA AAC GTC GAG GT-3, (antisense) 5-GCT GTG CAG GTG TTG AGC C-3 and Smad3 (sense) 5-AGG AAT TTG GTG CCC TCC TAG-3, (antisense) 5-GCC TTT GAC GAA GCT CAT GC-3.[21,25] RT-PCR for the hypoxanthine-guanine phosphoribosyltransferase (HPRT) (Rn01527838_g1) molecule was performed by using the Taqman real-time PCR assay (Applied Biosystem, Foster City, CA). The cycling conditions were as follows: 10 min at 95°C followed by 45 cycles at 20 sec each at 95°C, 58°C, and 72°C. ABI Prism 7700 Sequence Detection Software 1.9 (Applied Biosystems, Foster City, CA) was used for analysis. The mRNA expression was normalized relative HPRT expression.

Statistical analysis

The Sigma Stat© (SYSTAT Software Inc, Chicago, IL) software was used for statistical analysis. The data are reported as mean ± SEM. Tests for normality distribution were performed first, after which parametric (Student's t test) or nonparametric (Mann–Whitney test) tests were used. The level of statistical significance was $p < 0.05$.

Results

The four groups of rats did not differ significantly in terms of weight gain. In particular, the body weights at the end of the study of the UUO and UUO+L groups were 286.9 ± 18.0 and 256.7 ± 13.5 g, respectively.

Laser treatment ameliorates renal fibrosis

Histomorphometric analysis of the left renal tissue sections revealed that compared with the sham control animals, the percentage of fibrosis per field, quantified under polarized light, had increased markedly 14 days after UUO ($36.6 \times 10^{-3} \pm 6.5\%$ $vs.$ $184 \times 10^{-3} \pm 23.8\%$, $p < 0.001$). However, the intraoperative administration of LLLT significantly reduced this UUO-induced fibrosis ($98.5 \times 10^{-3} \pm 17.3\%$ $vs.$ $184 \times 10^{-3} \pm 23.8\%$, respectively, $p = 0.002$). Laser treatment without ureteral obstruction (the L group) did not induce any fibrosis (Fig. 2).

Effect of LLLT on EMT markers

The interstitial expression of α-SMA, constitutively expressed in smooth muscle cells of renal arterioles and myo-fibroblasts, a marker of EMT, was weak in the sham controls (0.2 ± 0.01% of the interstitial cortical area) and the L controls (0.14 ± 0.01%). By contrast, UUO markedly increased the interstitial α-SMA expression to 15.3 ± 1.1%. However, similar to our Sirius red-based analyses of renal fibrosis, intraoperative laser treatment significantly reduced the UUO-induced expression of this EMT marker on day 14 to 3.2 ± 0.4% (UUO+L vs. UUO $p < 0.001$) (Fig. 3).

FSP-1 is another marker of EMT that is normally expressed by fibroblasts but not by epithelial cells. There was little interstitial expression of FSP-1 in the sham and L groups (1.4 ± 0.1% and 2.9 ± 0.3% cells/field, respectively). By contrast, UUO elevated the number of interstitial FSP-1-positive cells to 22.5 ± 2.1 cells/field. However, intraoperative LLLT administration did not have a significant impact on this UUO-induced interstitial expression of FSP-1 (24.5 ± 1.7 cells/field; UUO vs. UUO+L, $p = 0.18$) (Fig. 4).

LLLT decreases the expression of pro-inflammatory and pro-fibrotic molecules

To examine the mechanisms that might be involved in the functional and histological protection observed in LLLT treatment animals, we analyzed the expression of pro-inflammatory and pro-fibrosis related molecules. After 14 days of obstruction, the UUO rats exhibited a striking upregulation of MCP-1 (8.71 ± 0.21 vs. 2.72 ± 1.09; UUO vs. Sham, $p = 0.006$) and IL-6 (24.59 ± 4.59 vs. 2.48 ± 1.62, UUO vs. Sham, $p = 0.01$). In the LLLT-treated animals, there was notably lower expression of the MCP-1 (5.34 ± 0.63 vs. 8.71 ± 0.21, UUO+L vs. UUO, $p = 0.008$) and IL-6 (8.92 ± 0.56 vs. 24.59 ± 4.59, UUO+L vs. UUO; $p = 0.02$) (Fig. 5A and B). Smad3 is important to mediate TGF-β1 action in inducting α-SMA expression. LLLT treatment significantly reduced the UUO-induced expression on day 14 (1.8 ± 0.2 vs. 2.93 ± 0.2, UUO+L vs. UUO, $p = 0.01$) (Fig. 5C). Although TGF-β1 exhibited a decrease in the LLLT group (UUO+L) this reduction did not show a statistical significance (2.96 ± 0.6 vs. 4.5 ± 0.65, UUO+L vs. UUO $p = 0.12$) (Fig. 5D).

Discussion

Here, we investigated, for the first time, the potential of LLLT to ameliorate fibrosis in a model of UUO. We did not find any reports of using laser therapy for this kind of kidney disease.

Laser radiation after UUO ameliorated several histological parameters, namely the degree of IF, the protein expression of α-SMA in the interstitium, and the mRNA expression of the pro-inflammatory and pro-fibrotic genes such as MCP-1, IL-6, Smad3 and TGF-β1 in the interstitium. Because treatment with LLLT attenuated all of these factors, it appears that LLLT can reduce obstruction-induced IF, at least in this model of CKD.

The experimental model of UUO does not reproduce all features seen in renal fibrosis in humans, but it is a fully reproducible model, widely used to study the cellular and molecular changes of the kidney upon ureteral obstruction.[21,26] These changes are well advanced within 10–14 days, a representative point of established lesion, with low mortality and morbidity.[19,26] In addition to providing a better understanding of the pathophysiology of renal fibrosis, the UUO model can be used to determine the treatments' efficacy to resolve fibrosis.[9]
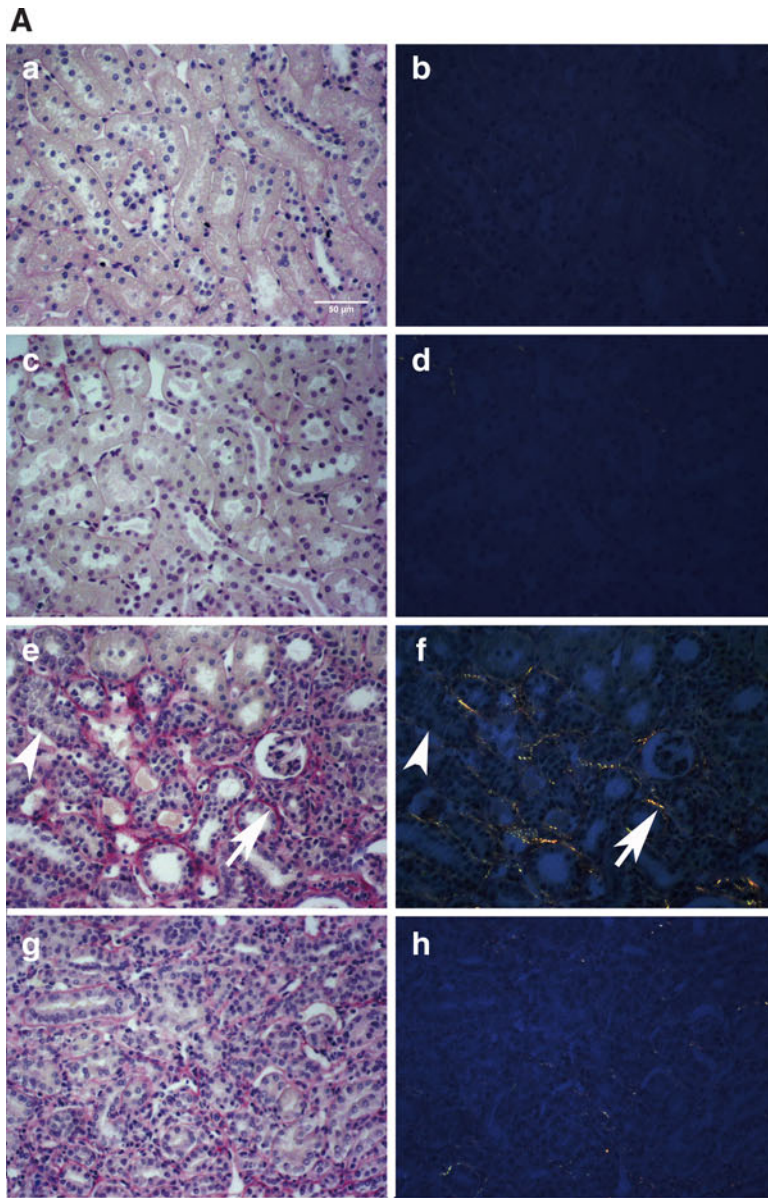
FIG. 2. Treatment with laser therapy reduces tubulointerstitial fibrosis in the obstructed kidney. **(A)** Sirius red staining of the sham control kidneys (Sham **a-b**), the low-level laser therapy (LLLT) alone kidneys (L, **c,d**), the unilateral ureteral obstruction (UUO) kidneys (**e,f**), and the LLLT-treated UUO kidneys (UUO+L, **g,h**). Panels **a, c, e,** and **g** show the tissue when seen under a light microscope, whereas panels **b, d, f,** and **h** show the same tissue under polarized light. **(e,f)** The large arrows indicate the birefringent Sirius red-stained molecules that correspond to collagens I or III, whereas the small arrows indicate the non-birefringent Sirius red-stained molecules that correspond to extracellular matrix components. **(B)** Graph of the fibrosis in the renal cortex expressed as percentage per examined field. The Sham and L groups had low interstitial fibrosis, but the rats subjected to UUO had highly marked interstitial fibrosis. The intraoperative administration of LLLT attenuated this UUO-induced fibrosis significantly. $*p < 0.001$ and $\#p = 0.002$; Sirius red, polarized light, five animals per group, 10 non-overlapping, $200 \times$ fields per animal.
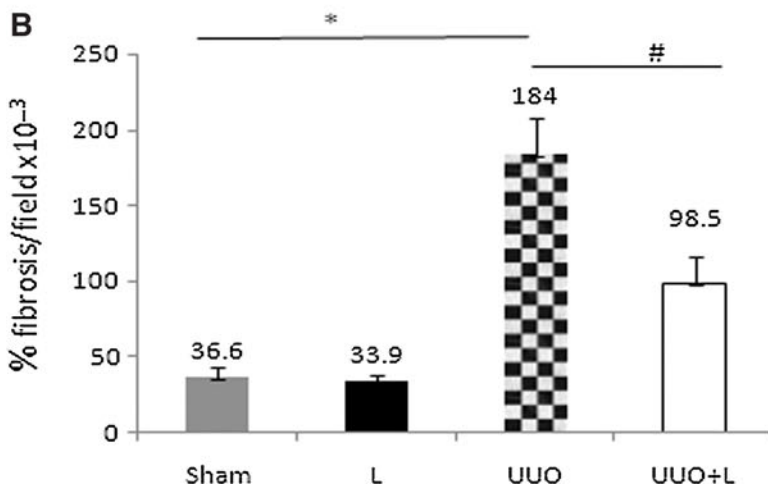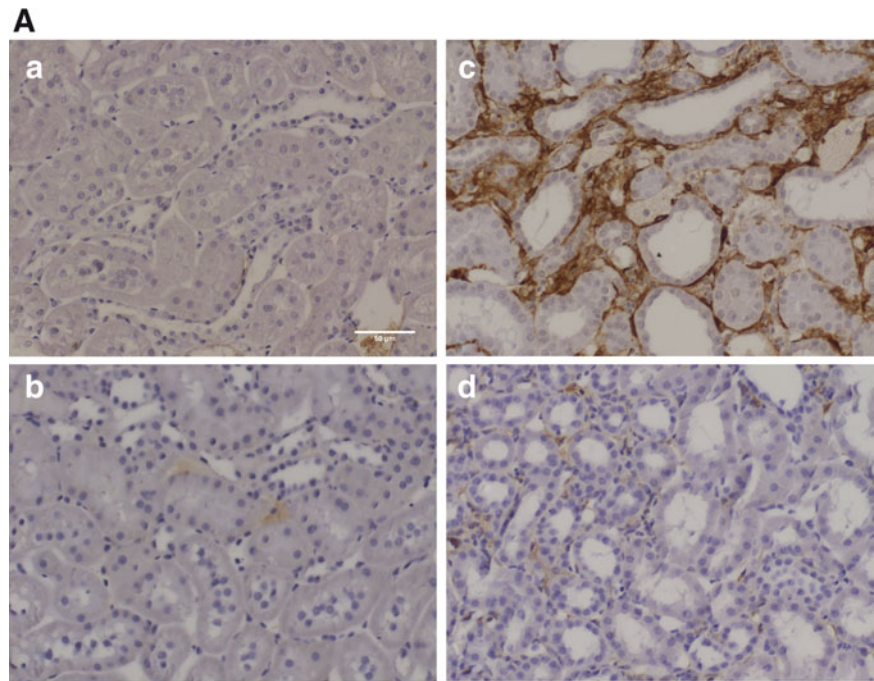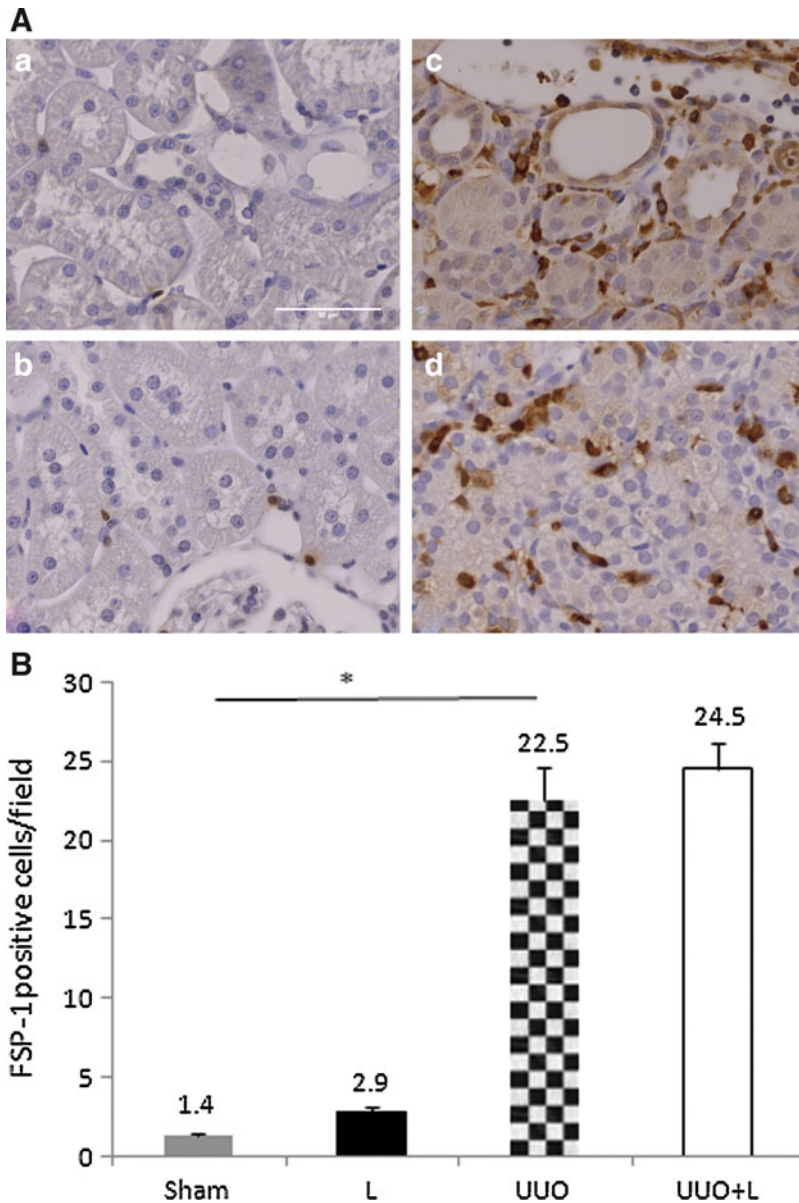
FIG. 3. Immunohistochemical localization of epithelial–mesenchymal transition (EMT) marker α-SMA. **(A)** Representative photomicrograph illustrating the α-SMA expression in the renal tissue after 14 days of obstruction. Compared with the laser-treated obstructed animals (**d**), the untreated obstructed animals exhibited larger interstitial accumulations of α-SMA-positive cells (**c**), as shown by DAB, a brown pigment. The Sham (**a**) and L (**b**) groups were very similar to each other in this regard. **(B)** Graph showing the α-SMA expression of all groups. In quantitative morphometric analysis, Sham and L groups presented a small percentage of interstitial α-SMA-positive area, whereas rats subjected to unilateral ureteral obstruction (UUO) showed a striking increase in interstitial positive cells. Laser administration significantly attenuated it. *$p < 0.001$ and #$p < 0.001$.
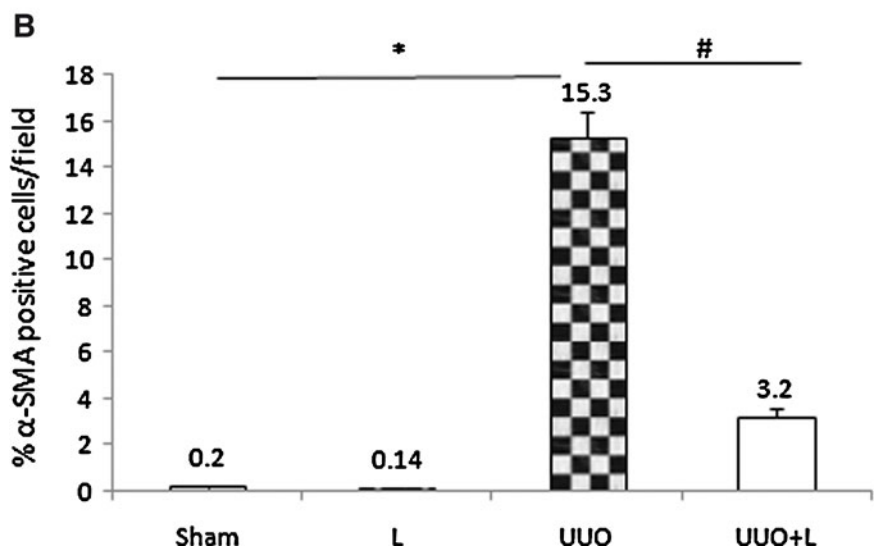
It remains unclear how infrared laser therapy improved the outcome of UUO in this study, but this type of irradiation has been documented to have positive effects on many organs and tissues.[14,15,18,27] Infrared irradiation's intrinsic mechanism may relate to an improvement in energy metabolism, cell viability is enhanced, and an attenuating in inflammation and fibrosis occurs in parallel.[18,21] Furthermore, relevant adverse outcomes attributed to the laser therapeutic procedures have not been reported.[12,15,28] However, most of the studies examining efficacy of LLLT treatment did not include a LLLT-only control group, which makes it difficult to investigate possible adverse outcomes of LLLT itself.[12,15] By contrast, in our study, the safety of laser therapy could be assessed because the L group was included. The Sirius red-stained areas of the kidney, α-SMA, pro-inflammatory genes and pro-fibrotic genes expression were similar to the sham group. Therefore, in the absence of the injury being investigated, LLLT appears to be safe.

Sirius red is a histochemical stain; when observed under polarized light only collagen types I and III are strongly birefringent.[29] In the present study, UUO induced advanced fibrosis, as demonstrated by Sirius red staining under polarized light. However, intraoperative LLLT reduced this fibrosis by 47%. The magnitude of fibrosis reduction, nearly twofold reduction, was described by other studies of OUU as a result of pharmacology intervention; in addition, they have analyzed a smaller area.[21,30] These findings correlate with a striking decrease, by 79%, of α-SMA-positive cells in laser-treated group. It should be noted that renal IF is a remarkably consistent process that does not vary regardless of the etiology: it always involves EMT, namely the *de novo*

A

B

FIG. 4. Immunohistochemical localization and quantification of FSP-1-positive cells (fibroblasts) in the interstitial renal cortex. **(A)** Compared with the Sham (**a**) and L controls (**b**), untreated unilateral ureteral obstruction (UUO) rats had higher numbers of fibroblast-specific protein-1 (FSP1)-positive cells in the interstitium (**c**). Laser treatment after UUO did not decrease these numbers significantly (**d**). The L animals exhibited higher numbers of FSP-1-positive cells (**b**) than did the Sham animals (**a**). **(B)** Graph showing the FSP-1 expression of all groups. UUO elevated the numbers of interstitial FSP-1-positive cells, but intraoperative laser administration did not reduce these numbers. $*p < 0.001$, sham versus UUO.

activation of α-SMA-positive myofibroblasts, which are the principal effector cells that are responsible for the excess deposition of interstitial ECM under pathological conditions.[1,4,6] Therefore, our findings suggest that LLLT reduces EMT, and consequently decreases renal fibrosis.

In some experimental studies, in different models, LLLT attenuates chronic histological features by preventing oxidative stress and inflammatory response.[15,18] Therefore, it is possible that the UUO + L group had smaller areas containing α-SMA injured myofibroblasts and less collagen deposition than the UUO group, because LLLT reduced the oxidative stress and the consequent inflammatory response after ureteral obstruction of the left kidney.[18,19,21] The observation that LLLT specifically blocks the activation of renal myofibroblasts *in vivo*, as well a direct evaluation of oxidative stress patterns, may provide major insights into the cellular mechanism underlying the amelioration of renal fibrotic lesions.

We also investigated the inflammation in kidney tissue by analyzing MCP-1 and IL-6. The recruitment of macrophages to the inflamed kidney depends upon the release of several chemokines, including MCP-1. In our study, whereas UUO elevated the MCP-1 expression in the kidney, in UUO animals that had been treated with LLLT, there was a significant reduction of MCP-1 by 38%. Other treatments have also been observed to have similar effects.[19,21,31] Moreover, LLLT treatment also drastically reduced in 63% the expression of IL-6 in UUO treated for LLLT, results also consistent with other studies.[21,32]

Because it is the main pro-fibrotic cytokine in renal fibrogenesis, we investigated the role of TGF-β1, and its cellular regulatory pathway, by expression of Smad3.[33,34] Previous studies have shown that the inhibition of TGF-β1 attenuates the renal interstitial fibrosis in UUO.[35,36] TGF-β1 mRNA expression in the UUO kidney was not significantly modified by LLLT in this model. Otherwise, this result was

FIG. 5. Semiquantitative reverse transcriptase polymerase chain reaction (RT–PCR) analysis of monocyte chemotactic protein-1 (MCP-1), interleukin-6 (IL-6), Smad3 and transforming growth factor-β1 (TGF-β1). (**A** and **B**) The obstructed kidneys (UUO) exhibited clear overexpression of MCP-1 and IL-6 compared with Sham. MCP-1, *$p < 0.05$ (UUO vs. Sham) and IL-6, *$p < 0.05$ (UUO vs. Sham). Intraoperative low-level laser therapy (LLLT) treatment (UUO+L) significantly decreased the expression of the former two molecules. MCP-1, *$p < 0.05$ (UUO+L vs. UUO) and IL-6, *$p < 0.05$ (UUO+L vs. UUO). (**C**) Laser administration significantly decreased the expression of the Smad3 compared with UUO. *$p < 0.05$ (UUO+L vs. UUO). (**D**) TGF-β1 exhibited an apparent decrease in the LLLT group (UUO+L) compared with the injury group (UUO) but this reduction was not statistically significant. Hypoxanthine-guanine phosphoribosyltransferase (HPRT) served as a housekeeping gene to ensure that the RNA content of the samples was similar.
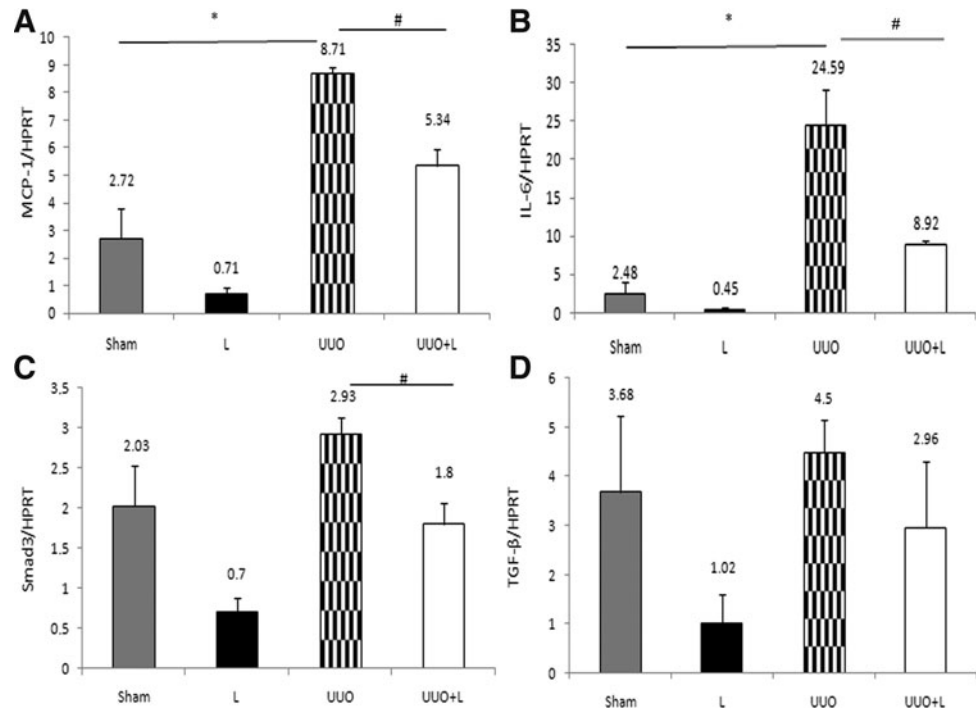
corroborated by the significant decrease of Smad3 mRNA expression. In addition, the fibrosis, as demonstrated by Sirius red staining under polarized light, was clearly downregulated. Alternatively, it has been demonstrated *in vitro* that MCP-1 has the ability to induce fibroblast to increase production of collagen through a mechanism independent of TGF-β1.[37] Therefore, it is conceivable that the MCP-1 expression could itself directly upregulate ECM compound production by fibroblasts, or activate tubular cells to transdifferentiate into fibroblast-like cells.

We noticed a significant increase in FSP-1 fibroblasts in obstructed kidney, but LLLT failed to promote a significant reduction in its amount. It does not correlate with our other findings. In addition, L group had significantly more cells that expressed FSP-1 than did the Sham group. Adult fibroblasts can be resident, derived from the bone marrow or by EMT.[38] In the present study, the fibroblasts that were present at higher numbers in the L group were supposed to be a consequence of LLLT action in the absence of UUO injury. Otherwise, they could be the type of mobile fibroblast that is responsible for the formation and structure of the tissue rather than the type of fibroblast that is generated by EMT and that is more heterogeneous and harmful.[39] Whereas fibroblast activation may be necessary for the development of full-scale renal interstitial fibrosis, it is not sufficient.[1] This is supported by the present study, because the FSP-1 levels of the UUO+L group did not differ significantly from those of the UUO group, despite the fact that the UUO+L group had significantly less fibrosis and fewer myofibroblasts. Therefore, it appears that LLLT-treated tissue may respond better to injury, thereby making its repair more structured, and then requiring a greater number of fibroblasts, and, perhaps, in a different time manner.[15,18]

Conclusions

In summary, the results indicate that LLLT markedly reduces the degree of tubule-interstitial fibrosis after induction of UUO in rats. The attenuation of fibrosis was associated with lower expression pro-inflammatory MCP-1, IL-6, and pro-fibrotic molecules Smad3 and TGF-β1. For our knowledge, it is the first description of such application for LLLT in kidney disease. These observations suggest that laser therapy could slow the progression of chronic renal injury. Moreover, we also realize that we need new technologies that improve the access of the laser radiation to the kidney to emerge, so laser therapy may also become useful for treating CKD in native and transplanted kidney patients.

Acknowledgments

Author Disclosure Statement

No conflicting financial interests exist.

References

1. Liu, Y. (2004). Epithelial to mesenchymal transition in renal fibrogenesis: pathologic significance, molecular mechanism, and therapeutic intervention. J. Am. Soc. Nephrol. 15, 1–12.

2. Bascands, J.L., and Schanstra, J.P. (2005). Obstructive nephropathy: insights from genetically engineered animals. Kidney Int. 68, 925–937.

3. Fujiu, K., Manabe, I., and Nagai, R. (2011). Renal collecting duct epithelial cells regulate inflammation in tubulointerstitial damage in mice. J. Clin. Invest. 121, 3425–3441.

4. Klahr, S., and Morrissey, J. (2003). Progression of chronic renal disease. Am. J. Kidney Dis. 41, S3–S7.

5. Wynn, T.A. (2008). Cellular and molecular mechanisms of fibrosis. J. Pathol. 214, 199–210.

6. Bani–Hani, A.H., Campbell, M.T., Meldrum, D.R., and Meldrum, K.K. (2008). Cytokines in epithelial-mesenchymal transition: a new insight into obstructive nephropathy. J. Urol. 180, 461–468.

7. Qi, W., Chen, X., Poronnik, P., and Pollock, C.A. (2006). The renal cortical fibroblast in renal tubulointerstitial fibrosis. Int. J. Biochem. Cell. Biol. 38, 1–5.

8. Favreau, F., Thuillier, R., Cau, J., et al. (2010). Anti-thrombin therapy during warm ischemia and cold preservation prevents chronic kidney graft fibrosis in a DCD model. Am. J. Transplant. 10, 30–39.

9. Klahr, S., and Morrissey, J. (2002). Obstructive nephropathy and renal fibrosis. Am. J. Physiol. Renal Physiol. 283, F861–F875.

10. Hruska, K.A. (2002). Treatment of chronic tubulointerstitial disease: a new concept. Kidney Int. 61, 1911–1922.

11. National Kidney Foundation (2002). K/DOQI clinical practice guidelines for chronic kidney disease: evaluation, classification and stratification. Am. J. Kidney Dis. 39, S1–S246.

12. Oron, A., Oron, U., Chen, J., et al. (2006). Low-level laser therapy applied transcranially to rats after induction of stroke significantly reduces long-term neurological deficits. Stroke 37, 2620–2624.

13. Rizzi, C.F., Mauriz, J.L., Freitas Correa, D.S., et al. (2006). Effects of low-level laser therapy (LLLT) on the nuclear factor (NF)-kappaB signaling pathway in traumatized muscle. Lasers Surg. Med. 38, 704–713.

14. Castro–e–Silva, O. Jr., Zucoloto, S., Marcassa, L.G., et al. (2003). Spectral response for laser enhancement in hepatic regeneration for hepatectomized rats. Lasers Surg. Med. 32, 50–53.

15. Oron, U., Yaakobi, T., Oron, A., et al. (2001). Low-energy laser irradiation reduces formation of scar tissue after myocardial infarction in rats and dogs. Circulation 103, 296–301.

16. Hu, W.P., Wang, J.J., Yu, C.L., Lan, C.C., Chen, G.S., and Yu, H.S. (2007). Helium-neon laser irradiation stimulates cell proliferation through photostimulatory effects in mitochondria. J. Invest. Dermatol. 127, 2048–2057.

17. Yaakobi, T., Shoshany, Y., Levkovitz, S., Rubin, O., Ben Haim, S.A., Oron, U. (2001). Long-term effect of low energy laser irradiation on infarction and reperfusion injury in the rat heart. J. Appl. Physiol. 90, 2411–2419.

18. Fillipin, L.I., Mauriz, J.L., Vedovelli, K., et al. (2005). Low-level laser therapy (LLLT) prevents oxidative stress and reduces fibrosis in rat traumatized Achilles tendon. Lasers Surg. Med. 37, 293–300.

19. Vieira, J.M.Jr., Mantovani, E., Rodrigues, L.T., et al. (2005). Simvastatin attenuates renal inflammation, tubular trans-differentiation and interstitial fibrosis in rats with unilateral ureteral obstruction. Nephrol. Dial. Transplant. 20, 1582–1591.

20. Oliveira, A.F., Silva, T.C., Sankarankutty, A.K., et al. (2006). The effect of laser on remanescent liver tissue after 90% hepatectomy in rats. Acta Cir. Bras. 21, 29–32.

21. Correa–Costa, M., Semedo, P., Monteiro, A.P., et al. (2010). Induction of heme oxygenase-1 can halt and even reverse renal tubule-interstitial fibrosis. PLoS One 5, e14298.

22. Grimm, P.C., Nickerson, P., Gough, J., et al. (2003). Computerized image analysis of Sirius Red-stained renal allograft biopsies as a surrogate marker to predict long-term allograft function. J. Am. Soc. Nephrol. 14, 1662–1668.

23. Semedo, P., Correa–Costa, M., Antonio Cenedeze, M., et al. (2009). Mesenchymal stem cells attenuate renal fibrosis through immune modulation and remodeling properties in a rat remnant kidney model. Stem Cells 27, 3063–3073.

24. Oliveira, R.S.F., Oliveira, F.A.M., e Pinheiro, H.S. (2010). Programming image software for automatic selection of immunohistochemistry marked areas stained by dab chromogen and counter-stained by hematoxylin. Rev. Interdisciplin. Est. Exp. Anim. Hum. 2, 76–80.

25. BLAST (Basic Local Alignment Search Tool) from The National Center for Biotechnology Information at www.blast.ncbi.nlm.nih.gov

26. Chevalier, R.L., Forbes, M.S., and Thornhill, B.A. (2009). Ureteral obstruction as a model of renal interstitial fibrosis and obstructive nephropathy. Kidney Int. 75, 1145–1152.

27. Santos, L.F., Carvalho, A. A., Leão, J.C., Cruz Perez, D.E., and Castro, J.F. (2011). Effect of low-level laser therapy in the treatment of burning mouth syndrome: a case series. Photomed. Laser Surg. 29, 793–796.

28. Vladimirov, Y.A., Osipov, A.N., and Klebanov, G.I. (2004). Photobiological principles of therapeutic applications of laser radiation. Biochemistry (Mosc) 69, 81–90.

29. Sweat, F., Puchtler, H., and Rosenthal, S.I. (1964). Sirius Red F3ba as a stain for connective tissue. Arch. Pathol. 78, 69–72.

30. Chen, C.O., Park, M.H., Forbes, M.S., et al. (2007). Angiotensin-converting enzyme inhibition aggravates renal interstitial injury resulting from partial unilateral ureteral obstruction in the neonatal rat. Am. J. Physiol. Renal Physiol. 292, F946–F955.

31. Belmiro, C.L., Goncalves, R.G., Kozlowski, E.O., et al. (2011). Dermatan sulfate reduces monocyte chemoattractant protein 1 and TGF-beta production, as well as macrophage recruitment and myofibroblast accumulation in mice with unilateral ureteral obstruction. Braz. J. Med. Biol. Res. 44, 624–633.

32. Matavelli, L.C., Huang, J., and Siragy, H.M. (2011). Angiotensin AT receptor stimulation inhibits early renal inflammation in renovascular hypertension. Hypertension 57, 308–313.

33. Sun, C.Y., Chang, S.C., and Wu, M.S. (2012). Uremic toxins induce kidney fibrosis by activating intrarenal renin-angiotensin-aldosterone system associated epithelial-to-mesenchymal transition. PloS One 7, e34026

34. Phanish, M.K., Wahab, N.A., Colville–Nash, P., Hendry, B.M., and Dockrell, M.E. (2006). The differential role of Smad2 and Smad3 in the regulation of pro-fibrotic TGFbeta1 responses in human proximal-tubule epithelial cells. Biochem. J. 393, 601–607.

35. Hwang, M., Kim, H.J., Noh, H.J., et al. (2006). TGF-beta1 siRNA suppresses the tubulointerstitial fibrosis in the kidney of ureteral obstruction. Exp. Mol. Pathol. 81, 48–54.

36. Kawai, T., Masaki, T., Doi, S., et al. (2009). PPAR-gamma agonist attenuates renal interstitial fibrosis and inflammation through reduction of TGF-beta. Lab. Invest. 89, 47–58.

37. Yamamoto, T., Eckes, B., and Krieg, T. (2001). Effect of interleukin-10 on the gene expression of type I collagen, fibronectin, and decorin in human skin fibroblasts: differential regulation by transforming growth factor-beta and monocyte chemoattractant protein-1. Biochem. Biophys. Res. Commun. 281, 200–205.

38. Li, M.X., and Liu, B.C. (2007). Epithelial to mesenchymal transition in the progression of tubulointerstitial fibrosis. Chin. Med. J. (Engl) 120, 1925–1930.

39. Kalluri, R., and Neilson, E.G. (2003) Epithelial-mesenchymal transition and its implications for fibrosis. J. Clin. Invest. 112, 1776–1784

Address correspondence to:
Helady Sanders-Pinheiro
Division of Nephrology
Universidade Federal de Juiz de Fora
Rua Benjamin Constant
1044/1001 Juiz de Fora
MG, 36015-400
Brazil

E-mail: helady.sanders@ufjf.edu.br